

Economic Optimization of Small Scale Organic Rankine Cycles

Bertrand F. Tchanche^a, S. Quoilin^b, S. Declaye^b, G. Papadakis^a and V. Lemort^b

^a Agricultural University of Athens, Athens, Greece

^b University of Liege, Liege, Belgium

Abstract: The present paper focuses on the economic optimization of a small scale ORC in waste heat recovery application with specific investment cost as objective function. First, a pre-design model of the ORC was built and simulations run with different working fluids to evaluate their technical performance. In a second step, components and system cost models were built and simulations carried out to evaluate the cost effectiveness of systems associated with different fluids. The working fluids considered are R245fa, R123, R113, n-Pentane and n-Butane. Results indicate that for the same fluid, the point of high performance and that of cost-effectiveness do not match. The operating point for maximum power doesn't correspond to that of the minimum specific investment cost. For n-Pentane, the maximum net power of 1.98 kW is obtained for an evaporator pressure of 5.14 bar and the specific investment cost is 5450 €/kW. For this same fluid, a minimum specific investment cost of 4440 €/kW is obtained for an evaporator pressure of 8.5 bar and the corresponding power output is 1.745 kW. The mismatch aforementioned is due to the thermodynamic properties such as liquid/vapour densities, which significantly influence system performance and components sizes. Seeking for profitable environmental solutions, economic optimization as a necessary step in the optimization of any thermodynamic system is highly advised.

Keywords: Economic Optimization, Organic Rankine Cycle, Waste Heat Recovery, Working Fluid.

1. Introduction

Modern societies depend critically on energy and continued economic growth requires further increases in energy consumption and energy demand. According to official reports on future global primary energy production and use, the high energy growth rates of the 20th century will continue unabated until 2050 and even beyond. Presently, the global primary energy use is roughly 500 EJ and shall double by 2050 [1]. The world economy heavily depends on fossil fuels (oil, coal and natural gas) which represent an 81% share of total primary energy use. Renewable energy and nuclear energy share the remainder, 13% and 6% respectively. Nevertheless, the fossil fuel-based economy raises a certain number of issues. The dramatic destruction of the environment attributed to the excessive use of fossil fuels has reached a critical level with unpleasant consequences [2]. Moreover, the fossil fuel resources are finite. Their future depletion results in a considerable increase in the energy price with undesirable shocks on the global economy. The growing concern for the supply and safe transportation of fossil fuels as well as the increase in the energy demand reinforce the scaling-up of fossil fuel prices and fuel international tensions.

Therefore, it is time to seek for alternate energy sources and to consider ways of saving the fast depleting fossil resources. Verbruggen [3] analyzed potential contenders for the future electricity supply from economic and sustainability viewpoints and proposed the twin efficiency/renewable power.

The Organic Rankine Cycles (ORC) as energy converter fall well in both sides of the twin. Their suitability in medium-scale power plants of few hundreds kW to MW power output has already been demonstrated in solar, geothermal, waste heat recovery and biomass power plants [4]. At the moment, there is a growing concern of recovering the heat wasted in industries during thermal processes as well as in thermal power plants and other thermal devices such as internal combustion devices. The potential for recovery is huge. For illustration, the analysis of manufacturing processes within the eight largest manufacturing sectors accounting for approximately 2/3 of the total energy used by the industrial sector in Canada showed that 70% (~1700 PJ) of the input energy was released to the environment [5].

Although investigated since the 1970s at the period of the oil crisis, the implementation of the recycling of the wasted energy for electricity generation has been

too slow or simply overlooked after the oil shocks as a result of the cheap fossil fuels prices. However, with growing concern on the environment and the fast depleting fossil fuels reserves, the interest on waste heat recovery for electricity is to know a new era. If the technology for medium and large scale ORCs is already mature, there is still room for research in small scale ORCs. In this perspective, a prototype of small scale ORC of few kWe was built and successfully tested at the University of Liège [6-8]. It uses R-245fa and R-123 as working fluids, and an oil-free scroll compressor adapted to run in expander mode. A thermodynamic model of the system was derived and validated for performance prediction. The validated thermodynamic model can be used to optimize the operation of the small ORC in waste heat recovery application. More recently, the economic evaluation of such small size systems was carried out to determine their cost effectiveness [9].

Most studies on ORCs as can be proven by the abundant relevant literature mainly focus on the optimization of the cycle efficiency and/or output power with respect to the cycle configuration and to the available working fluids [10-13]. Nevertheless, for the implementation of any new technology, the most important and determinant parameter is usually its affordability and not its performance. Thus, the present paper aims at performing the economic optimization instead of usual technical optimization. First, a pre-design model of the ORC is proposed and simulations are run with different working fluids candidates to evaluate their technical suitability. In a second step, components and system cost models are built and simulations run to evaluate the cost effectiveness of systems associated with different fluids. The working fluids used for the present study are: R245fa, R123, R113, n-Butane (R600) and n-Pentane (R601).

2. ORC in heat recovery application

The simple ORC system integrates four basic components: an evaporator, a turbine/alternator group, a condenser and a working fluid pump. Although many studies conclude that the introduction of regenerating processes (recuperator, feedliquid heater) increase the efficiency of the Rankine Cycle, the authors showed in a previous work that this is not justified in waste heat to power application for which the power output should be maximized instead of cycle efficiency [4]. The basic configuration is therefore selected in the present work. A heat source is needed to drive an ORC. Two ways exist to capture the wasted heat: (1) waste heat source and working

fluid exchange in the same heat exchanger and (2) a thermal oil loop is integrated to transfer the heat from the waste heat site to the evaporator. The configuration illustrated in Fig. 1 will be considered in the present study. Depending upon the condensing pressure, the hot water at the condenser outlet can be used for space heating or as domestic hot water. In some cases, dry cooling can be applied at the condenser to save the water resources. The electricity produced can be used on-site or sent to the grid as in case of renewable energy systems (solar PV, wind turbine, biomass or geothermal power plants).

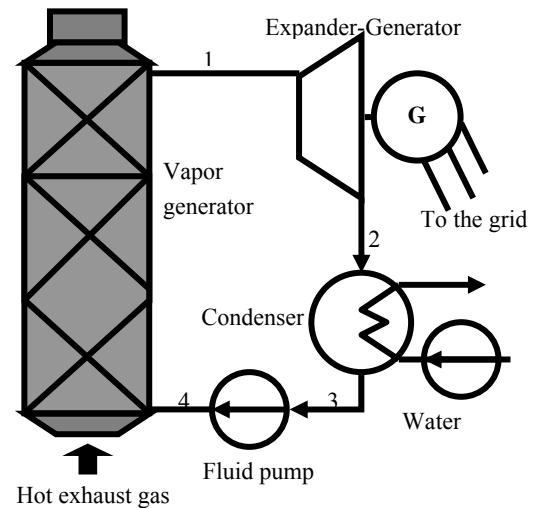


Fig.1. ORC in waste heat recovery application

3. Proposed fluid candidates

Selection of the most suitable working fluid is a critical step when designing an ORC. From numerous studies related to the selection of fluids for ORC-WHR, a certain number of criteria that should fulfil suitable fluids can be outlined. Fluids with high critical temperature or high boiling point such as toluene and silicone oils are adapted for high temperature heat sources. Hydrocarbons such as Pentanes, benzene, butanes and cryogenics such as R227ea, R123, R245fa, and HFE7000 are good candidates for moderate and low temperatures. Zeotropic mixtures were suggested for best matching with exhaust stream which leads to better operation of the heat exchangers and resource recovery. Fluids with a high vapour density are advisable as they allow reduction of vapour turbine size and heat exchangers areas. Presently, only a few working fluids are available on the market and some are being progressively phased out because of their harmful effects on the environment (high ODP) reducing the range of choice. In absence of specially designed

ORC fluids, any fluid used in other thermal processes as engineering fluids is welcome. Hence, there is a need to start designing specific fluids for ORCs as ORC will become an important technology for harnessing low grade heat in the next future. Nevertheless, some of fluids present on the market are giving satisfactory results. A quick screening of several potential fluids was done and those listed in Table 1 emerged as suitable and will be considered in the present study.

Table 1. List of considered working fluids

	$\rho_{\text{liq,wf}}$ (kg/m ³)	Tb (°C)	Tc (°C)	Pc (bar)
R-245fa	1352	15.3	154.1	36.4
R-123	1476.6	27.8	183.7	36.68
R-113	1574.9	47.6	214.1	34.39
R-600	625.7	-0.5	152	37.96
R-601	578.6	36.1	196.5	33.64
	UP _{wf} (€/kg)	ASHRA E 34	GWP	ODP
R-245fa	32	B1	820	0
R-123	15	B1	77	0.02
R-113	25	A1	6130	1
R-600	1.7	A3	0	0
R-601	1.7	A3	0	0

4. Modelling of a small scale ORC

The ORC model is built by interconnecting several models related to the components.

4.1. The scroll expander model

Volumetric expanders, such as scroll, screw or reciprocating technologies present an internal built-in volume ratio corresponding to the ratio between the inlet pocket volume and the outlet pocket volume.

Under-expansion occurs when the internal pressure ratio imposed by the expander is lower than the system pressure ratio. In that case, the pressure in the expansion chambers at the end of the expansion process (P_{in}) is higher than the pressure in the discharge line. *Over-expansion* occurs when the internal pressure ratio imposed by the expander is higher than the system pressure ratio. Under and over expansion losses can be modeled by splitting the expansion into two consecutive steps [14]:

1. Isentropic expansion:

$$w_1 = h_{\text{su}} - h_{\text{in}} \quad (1)$$

h_{in} being the isentropic enthalpy at pressure P_{in} .

2. Constant volume expansion:

$$w_2 = v_{\text{in}} (P_{\text{in}} - P_{\text{ex}}) \quad (2)$$

w_2 is positive in case of under-expansion, and negative in case of over-expansion (Fig. 2).

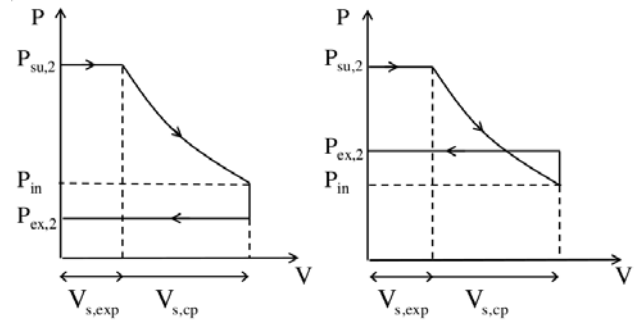


Fig. 2. Under and over-expansion losses

The total expansion work is then obtained by summing w_1 and w_2 . Other losses such as internal leakage, supply pressure drop, heat transfers and friction are lumped into one single mechanical efficiency η_{mech} . Thus, the actual expander work is expressed as:

$$\dot{W}_{\text{exp}} = \dot{M} (w_1 + w_2) \eta_{\text{mech}} \quad (3)$$

For given rotational speed and fluid flow rate, the expander imposes the evaporating pressure. This is computed by:

$$\dot{M} = \frac{\text{FF} \cdot \rho_{\text{su}} \cdot V_s \cdot N_{\text{rot}}}{60} \quad (4)$$

4.2. The heat exchanger model

The condenser and the evaporator are modelled using the ϵ -NTU method for counter-flow heat exchangers. The heat exchanger is divided into three zones (Fig. 3)[7]: a liquid zone, a two-phase zone and a vapour zone. Each zone is characterized by the heat transfer area A and a heat transfer coefficient U . The heat transfer coefficient U is given by $1/U = 1/h_r + 1/h_{\text{sf}}$.

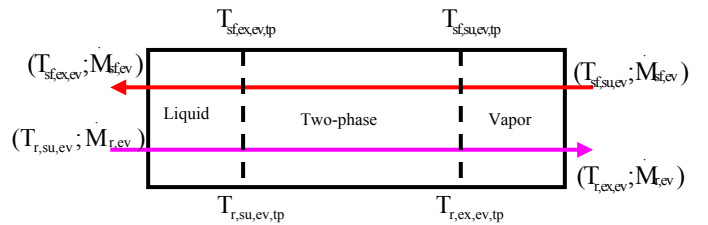


Fig.3. Three-zone model of the heat exchangers

4.3. The pump model

The pump is characterized by its swept volume and its global isentropic efficiency. Its electrical consumption is calculated using the relation

$$\dot{W}_{el,p} = \dot{V}_{s,p} (P_{r,ex,p} - P_{r,su,p}) / \eta_p \quad (5)$$

In the latter model (Fig. 4), the mass flow rate displaced by the pump depends on the pump capacity and swept volume.

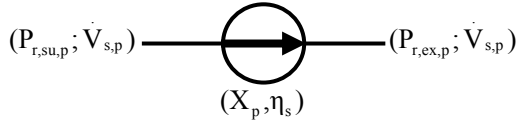


Fig. 4. Pump model

4.4. The global model

The global model of the ORC is built by interconnecting the models of different components above described to predict the system power output and cycle efficiency.

5. Thermodynamic optimization

5.1. Scope and method

The performance of a small scale ORC is predicted using the global model described in the previous section. Using that global model, the performance of the small scale ORC can be predicted. In the present case of an ORC in waste heat recovery application, the thermodynamic optimization aims at maximizing the net power output. However, other thermodynamic parameters can be used to characterize the thermodynamic behaviour of the system and are described in the following lines.

The cycle thermal efficiency is an indicative parameter of the quantity of heat converted into power and is given by:

$$\eta_{ORC} = (\dot{W}_{sh} - \dot{W}_p) / \dot{Q}_{ev} \quad (6)$$

The recuperation efficiency is the ratio of the heat recovered to the maximum heat recoverable. It can thus be written as

$$\varepsilon_R = \frac{\dot{Q}_{ev}}{\dot{Q}_{ev,max}} = \frac{\dot{M}_a c_{p,a} (T_{su,a} - T_{ex,a})}{\dot{M}_a c_{p,a} (T_{su,a} - T_{amb})} = \frac{T_{su,a} - T_{ex,a}}{T_{su,a} - T_{amb}} \quad (7)$$

The global energy conversion efficiency is the product of the cycle thermal efficiency and the recuperation efficiency.

$$\eta_{global} = \varepsilon_R \eta_{ORC} \quad (8)$$

For an ORC in which the heat source experiences a high decrease in temperature when it is cooled down during the heat recovery process, it is not convenient

to use the Carnot efficiency [15]. This is applicable to ORCs in geothermal and heat recovery applications. Instead of being defined from the rectangular cycle, the maximum cycle efficiency is derived from the triangular cycle and the triangular or trilateral efficiency is obtained. It is given by

$$\eta_{TR} = (T_{a,su} - T_{w,su}) / (T_{a,su} + T_{w,su}) \quad (9)$$

The ratio of the cycle thermal efficiency to the triangular efficiency called “relative trilateral efficiency” can be derived from equations 6 and 9 and expressed as

$$\eta_{TR-ORC} = \eta_{ORC} / \eta_{TR} \quad (10)$$

For the present study, many assumptions are made:

- The heat source is exhaust gas at 180 °C, assimilated to hot air with a mass flow rate of 0.21 kg/s.
- The condenser is cooled with cold water at 10 °C.
- The pinch point at the evaporator is 15 K.
- The pinch point at the condenser is 10 K.
- The superheating at the expander inlet, 5 K.
- The subcooling after the condenser, 5 K.
- The volumetric ratio of the scroll expander, 3.4.
- Expander mechanical efficiency, 70%.
- The isentropic efficiency of the pump, 60%.

The ORC global model was implemented in EES (Engineering Equation Solver) and the behavior of the system simulated under various conditions to find the optimal operation point. Fig. 5 shows the T-s diagram of the ORC with R123 as working fluid.

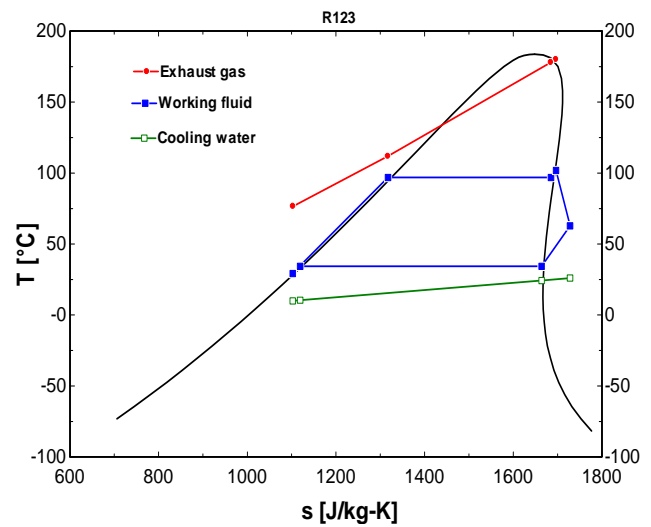


Fig.5. Temperature-entropy diagram with superposed heat source and heat sink profiles

Figs 6, 7 and 8 show the evolution of different parameters related to the system under different

evaporator pressure at which heat is transferred to the power cycle. From Fig. 6, it can be seen that an increase in evaporator pressure reduces the amount of heat transferred to the cycle and the amount of heat rejected at the condenser. The reduction of the amount of heat captured in the evaporator affects the temperature of the exhaust effluent/gas rejected to the environment; its temperature increases.

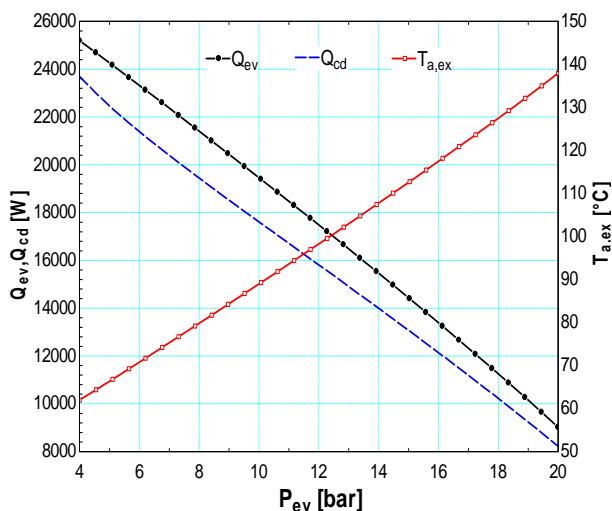


Fig. 6. Heat input, Heat rejected and temperature of the rejected exhaust

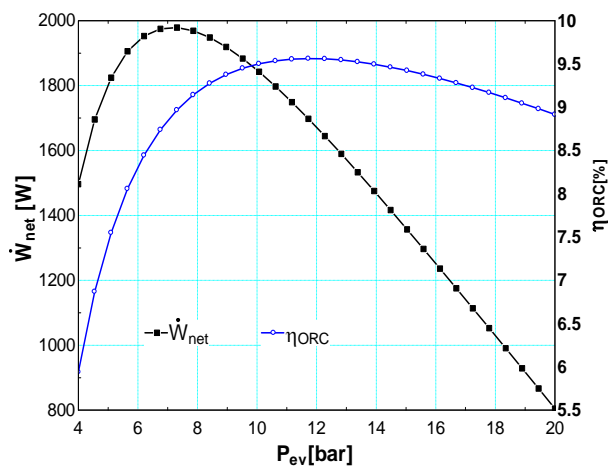


Fig. 7. Net power output and cycle efficiency

Fig. 7 shows the evolution of the net power output and cycle thermal efficiency. An optimum is obtained for both parameters but at different pressure values. The maximum net power of 1.80 kW is obtained for 7.31 bar while the maximum cycle efficiency (9.63%) is observed when the pressure reaches 11.72 bar. The maximum cycle efficiency is explained by under-expansion losses in the expander that increase when the pressure ratio is increased. In the case of heat

recovery, since the heat source is free, the output power and not the cycle efficiency should be maximized.

Fig. 8 shows the evolution of the recuperation efficiency, cycle thermal efficiency, cycle relative trilateral efficiency and global efficiency. The recuperation efficiency decreases linearly as the evaporator pressure increases. The global efficiency has a maximum (5.45%) at about 7.31 bar and the same trend as the net power output. Both cycle efficiency and relative trilateral efficiency have the same evolution. They increase progressively and reach a maximum at about 11.72 bar and decrease slightly afterwards. The cycle maximum efficiency and relative trilateral efficiency are 9.56% and 41.4% respectively.

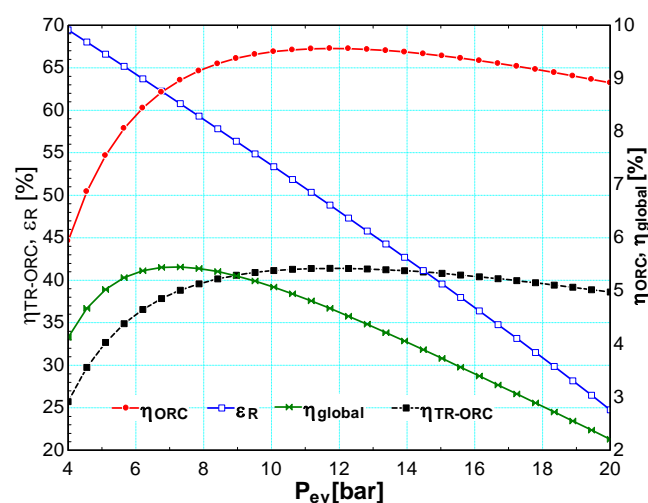


Fig. 8. Cycle, recuperation and global efficiency

5.2. Fluid comparison

Most criteria that should fulfil suitable working fluids in ORCs are well established [16]. These are: adequate critical parameters, high liquid and vapour densities, good thermal stability and compatibility with materials, appreciable safety characteristics, market availability and low cost, good thermodynamic performance and low environmental impact. The fluids in Table 1 will be considered further. The critical parameters for all fluids are suitable for subcritical cycles with the temperature of the heat source used. The thermal stability is not questionable for the considered fluids since the evaporating temperature does not exceed 200 °C. From compatibility point of view, only R123 is questionable as its corrosiveness has been reported. This can be solved by good selection of materials. All fluids proposed are available on the market with

different prices as displayed in Table 1. Hydrocarbons are abundant at very cheap prices. Among the fluids proposed, R113 has a high ODP (1) and a high GWP (6130) and is phased-out in developed countries. N-Pentane and n-Butane raise the issue of flammability. Nevertheless, they can be considered as low risks substances as they are becoming familiar in domestic appliances. R245fa and R123 are toxic substances requiring special attention from the operator during manipulation. Performance parameters of ORCs associated with different fluids after power output optimization are displayed in Table 2. The evaporating pressures recorded are well below the maximum acceptable limit of 25 bar. Both R245fa and n-Butane yield higher output and require high evaporating pressure. R245fa despite its toxicity has the highest vapour density at the expander inlet which would mean small expander. On the other hand, n-Butane is flammable but a very low cost fluid with the highest maximum power output. At this step, only a deep economic analysis could determine which one is to be selected.

Table 2. Thermodynamic parameters at maximum net power output

Fluids	P_{ev} (bar)	W_{net} (W)	$\rho_{p,su}$ (kg/m ³)	$\rho_{exp,su}$ (kg/m ³)
R245fa	11.79	2004	1324	64.98
R123	7.31	1979	1453	42.59
R113	3.93	1942	1554	26.42
n-Pentane	5.14	1979	616.6	13.78
n-Butane	15.31	2078	567.3	38.04

6. Economic optimization

6.1. Cost modelling

6.1.1. Expander cost model

For recall, the present expander is a scroll compressor adapted to run in reverse mode. The size of the compressor is linked to the thermodynamic characteristics of the fluid (density, volume flow rate) at the compressor outlet which corresponds to the expander inlet. From a catalogue of scroll hermetic compressors, and taking into account the cost of transformation, the expander cost is a linear function of the expander inlet volume flow rate:

$$C_{exp} = 450 + 340 \dot{V}_s \quad (11)$$

6.1.2. Heat exchanger cost model

Heat exchangers are characterized by the heat exchange surface area which is one of parameters that determine the quantity of heat recuperated or rejected.

For the present study, the cost model for heat exchangers deducted from a catalogue of flat plate heat exchangers is a linear function of the heat exchanger area:

$$C_{hx} = 388 + 480 A_{hx} \quad (12)$$

6.1.3. Pump cost model

Suitable pumps for small scale ORCs are small reciprocating pumps which can suck the liquid fluid at a pressure around 2-5 bar and deliver pressurized liquid fluid at about 10-20 bar while consuming small power input. However, it should be mentioned that there is no pump designed for liquid refrigerants. The cost model used in the present study is based on the relation between the power consumption and the cost as proposed by Bejan et al. [17]:

$$C_p = C_{p,ref} (\dot{W}_p / \dot{W}_{p,ref})^m \quad (13)$$

$m=0.25$ for small reciprocating pumps (<300 W), and $m=0.45$ when the input power exceeds 300 W. From the offers obtained from suppliers in Liege, Belgium, the reference pump considered has a power input of 300 W and costs 900 €.

6.1.4. Pipes cost model

Given the same length, pipes are characterized by their diameter. In the present study, liquid and vapour pipes are distinguished and have different diameters. Depending upon the fluid, for the same state of fluid the diameter may differ. From offers of suppliers in Liege, Belgium, the cost model for pipes is a linear function of the diameter:

$$C_{pp} = -6.90 + 6.75 D_{pp} \quad (14)$$

6.1.5. Fluid cost model

After examination of different prices of working fluids available on the market, it was difficult to build a correlation between the cost and thermodynamic characteristics. However, knowing the fluid charge, the cost of the working fluid for a particular system can be evaluated using the following relation:

$$C_{wf} = V_{liq,wf} \cdot UP_{wf} \cdot \rho_{liq,wf} \quad (15)$$

Where $V_{liq,wf}$ is the fluid charge; UP_{wf} , the unit price of the fluid and $\rho_{liq,wf}$, the density of liquid fluid.

The working fluid charge can be calculated based on the assumption that only the liquid part of the circuit is considered [18]; this is justified by the difference in density between vapor and liquid phases. The density of the fluid in liquid phase is much greater than the density in vapor state. Accordingly, the volume of the expander and the volume of vapor pipes as well as

parts of heat exchangers are not taken into account. Thus, the liquid volume consists of $\frac{3}{4}(\frac{1}{2})$ of the evaporator volume, $\frac{1}{4}(\frac{1}{2})$ of the condenser volume, swept volume of the pump, liquid pipes volume and liquid reservoir volume.

$$V_{liq,wf} = (3/8)V_{ev} + (1/8)V_{cd} + V_{s,p} + V_{liq,pp} + V_{lr} \quad (16)$$

6.2. Influence of the working conditions

The cost models in the previous section (6.1) show that the costs of components are linked to the geometry/size of the components which in fact depends on the thermodynamic characteristics of the working fluid used. To appreciate the influence of the thermodynamic characteristics R123 will be used.

Fig. 9 shows the variation of the costs of the heat exchangers and the working fluid with the evaporating pressure. The cost of the condenser decreases linearly as the evaporating pressure increases. Fluid and evaporator costs present the same trend as power output. They increase, reach a maximum at about 7.31 bar and decrease as the pressure increases. The decrease with the above items is due to the reduction of the heat exchanger area which reduces as the evaporating pressure is increased.

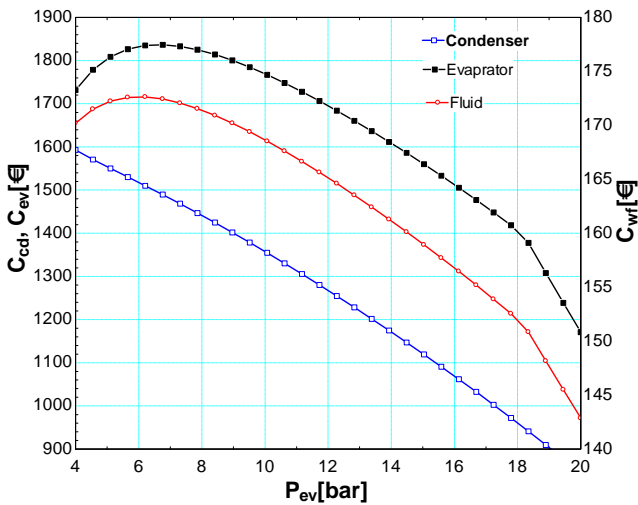


Fig. 9. Variation of the heat exchangers and working fluid costs with the evaporator pressure

In Fig. 10 can be appreciated the cost evolution of active components with evaporating pressure. With neglected pressure drop in the evaporator, evaporating pressure is the discharge pressure for the pump and the inlet pressure for the expander. The pump cost increases progressively, reaches a maximum at about 14 bar while the expander cost decreases gradually. The variations observed for both components are due to the density of the fluid at different states. For the

same pressure, one discharges pressurized liquid while the other sucks superheated vapour.

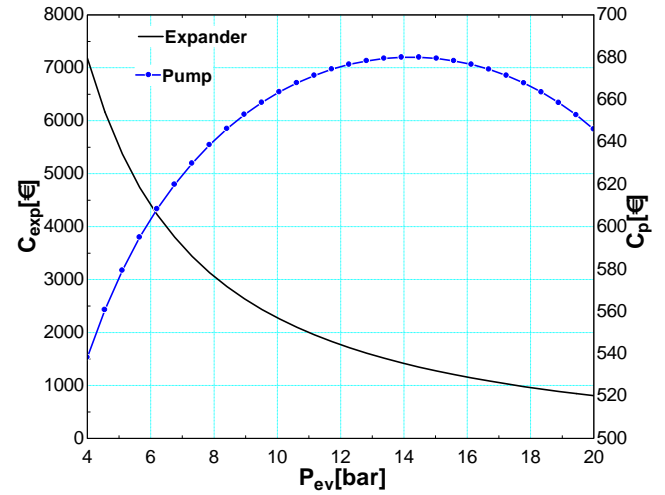


Fig. 10. Variation of the pump and expander costs with the evaporator pressure

6.3. Cycle cost model

In the previous section (6.2) it was seen that different components have different cost variations depending upon the working condition. This section aims at summing all components costs to build the total investment cost (TIC) and the specific investment cost (SIC). The TIC is the sum of various costs [9]:

- Scroll expander,
- Evaporator,
- Condenser,
- Fluid pump,
- Pipes,
- Working fluid charge,
- Other equipments: water cooling pump (300 €), liquid reservoir (200 €), control system (500 €) and miscellaneous hardware (300 €) for which the costs are neither dependant of fluids nor its thermodynamic state.
- The labour cost (10% of the total equipment cost).

$$TIC = \sum_{i=1}^n C_i \quad (17)$$

The specific system investment cost can be deduced:

$$SIC = TIC / \dot{W}_{net} \quad (18)$$

On Fig. 11, the evolution and weight of different components on the TIC are shown for R123. As can be seen, the most expensive components are the expander and the heat exchangers. The share of the expander compared to the total cost is particularly

important at pressures below 11 bar, then decreases while the share of heat exchangers increases. This is due to the decrease of heat exchangers cost in narrow ranges. The influence of the working fluids and pipes are almost negligible. However, the overall cost of the ORC decreases with an increase in evaporating pressure.

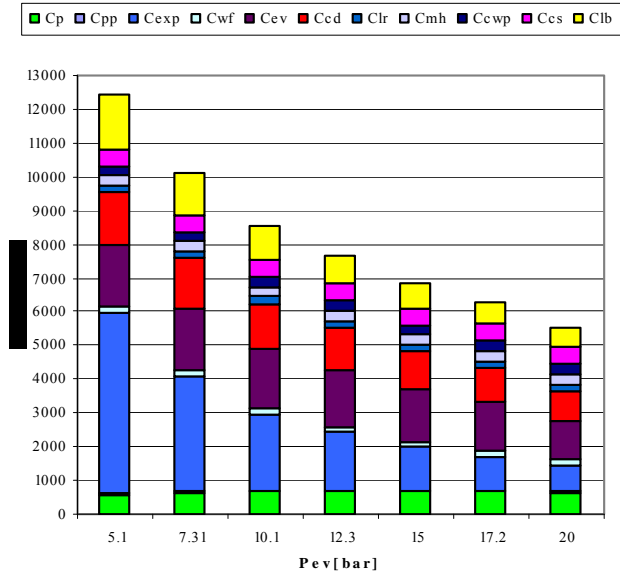


Fig. 11. Contribution of individual cost components on the TIC with R123 as working fluid

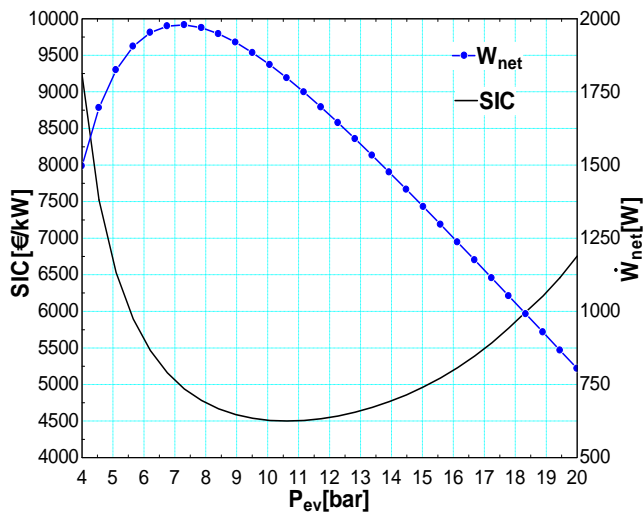


Fig. 12. Minimum SIC and Maximum net power

The specific investment/installed cost for any electricity generating system is a good indicator its cost effectiveness as it associates the investment with the capacity/performance. On Fig. 12, the evolution of the SIC with the evaporating pressure is depicted. A minimum value for the SIC is observed. For the case of R123 used here, this minimum occurs at an

evaporating pressure of 10.62 bar. However, this minimum does not coincide with maximum power of 1979 W obtained at 7.31 bar. This observation can be extended to other fluids used in this investigation.

6.4. Cost optimization

The selected objective function for this optimization is the specific investment cost (SIC) expressed in €/kWe. Since WHR sources are cost-free by definition, optimizing this parameter is equivalent to optimizing the profitability of the system if maintenance and insurance annual costs are neglected. For a given working fluid, several different working conditions can be optimized. The evaporating pressure shows an optimum in terms of overall efficiency and also in terms of profitability. The pinch point on the heat exchangers also shows an optimum value: the lower this value, the higher the cycle efficiency but the higher the heat exchange area and the higher the cost. The choice of the pinch point value therefore results of a thermo-economic optimization of the system. Three parameters (P_{ev} , $\Delta T_{pp,cd}$, $\Delta T_{pp,ev}$) are therefore to be optimized with the objective of minimizing the SIC. This is done using the simplex algorithm [19]. The results of the optimization for each fluid are presented in Table 3. Table 4 shows results for maximum power for comparison.

Table 3. Three-parameters optimization of the SIC

Fluids	$\Delta T_{pp,cd}$ (K)	$\Delta T_{pp,ev}$ (K)	P_{ev} (bar)	W_{net} (W)	SIC (€/kW)
R245fa	15.66	18.58	15.50	1720	4413
R123	15.46	12.54	11.31	1750	4361
R113	17.92	10.7	7.39	1586	5128
n-Pentane	15.17	12.66	8.5	1745	4440
n-Butane	14.51	17.3	19.7	1816	3869

Table 4. One-parameter optimization of the net power output for $\Delta T_{pp,cd}=10$ K and $\Delta T_{pp,ev}=15$ K

Fluids	P_{ev} (bar)	W_{net} (W)	TIC (€)	SIC (€/kW)
R245fa	11.79	2004	9533	4757
R123	7.31	1979	9775	4939
R113	3.93	1942	12485	6430
n-Pentane	5.14	1979	10784	5450
n-Butane	15.31	2078	8475	4078

From Tables 3 and 4, it is seen that there is no fluid for which the minimum SIC and maximum net power coincide. For all fluids, increasing the evaporating pressure by about 3.5 bar from the point of maximum power, results in a loss in power and gain in specific cost reduction. The extent in the SIC reduction depends on the fluid. The economic optimization offers different results for different fluids. The SIC reduction is about 5.12% for n-Butane, 7.23% for R245fa, 11.70% for R123, 18.53% for n-Pentane and 20.25% for R113. Globally power loss of 200-400 W generates cost reduction from 1500 up to 4500 €. Transforming the reduction in SIC into net power and TIC reduction; 18.33% reduction in power leads to 34.85% of gain in TIC for R113. Table 3 shows that the optimum pinch point values for both the evaporator and the condenser are comprised between 10 and 20K, which could therefore be considered as reference values regarding the economical optimum for this kind of application.

7. Conclusion

The increase of the share of renewable energy in the global primary energy mix is slowed by the cheap fossil fuels although they have been recognized as a major treat to our environment. In the transition to the renewable energy era, efficiency through waste heat recovery has a role to play. ORC in waste heat recovery application better needs to be cost-effective than efficient. In the study performed, a pre-design model of the ORC was built and simulations run with different working fluids to evaluate their technical performance. Components and system cost models were built and simulations carried out to evaluate the cost effectiveness of systems associated with different fluids. Results indicate that efficient and cost-effective systems do not match. The mismatch is due to very different thermodynamic properties such as liquid/gas densities, which significantly influence system performance and components sizes. In the case of R113, a loss of 356 W on power output leads to a saving of 4352 € on total investment cost. The role of the pinch points on heat exchangers was also underlined. Good values are taken between 10-20 K. Seeking for profitable environmental solutions; economic optimization instead of thermodynamic optimization is advisable.

Nomenclature

A	Area (m ²)
C	Cost (€)
D	Diameter (cm)

FF	Filling factor (-)
h	Heat transfer coefficient (W/m ² K)
M	Mass flow rate (kg/s)
N	Rotational speed (tr/min)
P	Pressure (bar)
Q	Thermal heat (W)
T	Temperature (°C, K)
U	Global heat transfer coefficient (W/m ² K)
V	Volume flow rate (m ³ /s)
W	Power output (W)
X	Capacity (-)
	<i>Greek symbols</i>
ε	Recuperation efficiency (%)
η	Thermal or global efficiency (%)
ρ	Density (kg/m ³)
	<i>subscripts</i>
a	air/exhaust gas
amb	ambient
c	critical
cd	condenser
cs	control system
cwp	cooling water pump
ev	evaporator
ex	exit
hx	Heat exchanger
lb	labour
leak	leakage
liq	liquid
loss	losses
lr	Liquid reservoir
m	maximum
mech	mechanical
mh	Miscellaneous hardware
r	working fluid
p	pump
pp	pipe
s	isentropic
sh	shaft
su	supply
sf	secondary fluid
TR	trilateral or triangular
w	water
wf	working fluid

REFERENCES

- [1] Moriarty, P., Honnery, D., 2009, What energy levels can the Earth sustain?, Energy Policy (37), pp. 2469-2474.
- [2] Sims, R.E.H., 2004, Renewable energy: a response to climate change, Solar Energy (76), pp. 9-17.

- [3] Verbruggen, A., 2008, Renewable and nuclear power: A common future?, *Energy Policy* (36), pp. 4036-4047.
- [4] Quoilin, S., and Lemort, V., 2009, Technological and Economical Survey of Organic Rankine Cycle Systems, In *Proceedings of the 5th European Conference on Economics and Management of Energy in Industry*, April 2009.
- [5] Galanis, N., Cayer E., Roy, P., Denis E.S, Desilets M., 2009, Electricity Generation from Low temperature sources, *Journal of Applied Fluid Mechanics* (2), pp. 55-67.
- [6] Declaye S, 2009. Design, optimization and modeling of an organic Rankine cycle for waste heat recovery, MSc Thesis, University of Liege.
- [7] Quoilin, S., Lemort, V., Lebrun, J., 2010, Experimental study and modeling of an Organic Rankine Cycle using scroll expander. *Applied Energy* (87), pp. 1260-1268.
- [8] Lemort V., Quoilin, S., Cuevas, C., Lebrun, J., 2009, Testing and modelling a scroll expander integrated into an Organic Rankine Cycle, *Applied Thermal Engineering* (29), pp. 3094-3102.
- [9] Tchanche, B.F., Quoilin, S., Declaye S., Papadakis, G., Lemort, V., 2010, Economic feasibility study of a small scale organic Rankine cycle system in waste heat recovery application, in *Proceedings of ESDA 2010*, July 12-14, Istanbul, Turkey.
- [10] Tchanche, B.F., Papadakis, G., Lambrinos, Gr., Frangoudakis, A., 2008, Effects of regeneration on low temperature solar organic Rankine cycles, in *Proc. of Eurosun 2008*, 7-10 October, Lisbon, Portugal.
- [11] Badr, O., Probert, S.D., O'Callaghan, P.W., 1985, Selecting a working fluid for a Rankine-Cycle Engine, *Applied Energy* (21), pp.1-42.
- [12] Tchanche, B.F., Papadakis, G., Lambrinos, G., A. Frangoudakis, 2009, Fluid selection for a low-temperature solar organic Rankine cycle, *Applied Thermal Engineering* (29), pp. 2468-2476.
- [13] Dai, Y., Wang, J., Gao, L., 2009, Parametric optimization and comparative study of organic rankine cycle (ORC) for low grade waste heat recovery, *Energy Conversion and Management* (50), pp.576-582.
- [14] Zanelli, R., Favrat, D., 1994, Experimental Investigation of a Hermetic Scroll Expander-Generator, *Proceedings of the 12th International Compressor Engineering Conference at Purdue*, pp. 459-464.
- [15] DiPippo R, 2007, Ideal thermal efficiency for geothermal binary plants, *Geothermics* (36), pp. 276-285.
- [16] Tchanche, B.F., Papadakis, G., Lambrinos, Gr., Frangoudakis, A., 2008, Criteria for working fluids selection in low temperature solar organic Rankine cycles, in *Proc. of Eurosun 2008*, 7-10 October, Lisbon, Portugal.
- [17] Bejan, A., Tsatsaronis, G., Moran, M., 1996, *Thermal Design and Optimization*, John Wiley & Sons.
- [18] Quoilin, S., 2007, Experimental Study and Modeling of a Low Temperature Rankine Cycle for Small Scale Cogeneration, MSc Thesis, University of Liege.
- [19] Nelder J. A., Mead, R., 1965, A simplex method for function minimization", *Computer Journal*, vol 7, pp. 308-313